Skeletal PET with ^{18}F-Fluoride: Applying New Technology to an Old Tracer*

Frederick D. Grant[1,2], Frederic H. Fahey[1,2], Alan B. Packard[1,2], Royal T. Davis[1], Abass Alavi[3,4], and S. Ted Treves[1,2]

[1]Division of Nuclear Medicine/PET, Children's Hospital Boston, Boston, Massachusetts; [2]Harvard Medical School, Boston, Massachusetts; [3]Division of Nuclear Medicine, Hospital of the University of Pennsylvania, Philadelphia, Pennsylvania; and [4]University of Pennsylvania Medical School, Philadelphia, Pennsylvania

Although ^{18}F-labeled NaF was the first widely used agent for skeletal scintigraphy, it quickly fell into disuse after the introduction of ^{99m}Tc-labeled bone-imaging agents. Recent comparative studies have demonstrated that ^{18}F-fluoride PET is more accurate than ^{99m}Tc-diphosphonate SPECT for identifying both malignant and benign lesions of the skeleton. Combining ^{18}F-fluoride PET with other imaging, such as CT, can improve the specificity and overall accuracy of skeletal ^{18}F-fluoride PET and probably will become the routine clinical practice for ^{18}F-fluoride PET. Although ^{18}F-labeled NaF and ^{99m}Tc-diphosphonate have a similar patient dosimetry, ^{18}F-fluoride PET offers shorter study times (typically less than 1 h), resulting in a more efficient workflow, improved patient convenience, and faster turnarounds of reports to the referring physicians. With the widespread availability of PET scanners and the improved logistics for the delivery of ^{18}F radiopharmaceuticals, prior limitations to the routine use of ^{18}F-fluoride bone imaging have largely been overcome. The favorable imaging performance and the clinical utility of ^{18}F-fluoride PET, compared with ^{99m}Tc-diphosphonate scintigraphy, support the reconsideration of ^{18}F-fluoride as a routine bone-imaging agent.

Key Words: ^{18}F-labeled sodium fluoride, skeletal PET

J Nucl Med 2008; 49:68–78
DOI: 10.2967/jnumed.106.037200

Several decades before the introduction of modern PET systems, ^{18}F-labeled NaF was recognized as an excellent radiopharmaceutical for skeletal imaging (*1*). ^{18}F-Fluoride has the desirable characteristics of high and rapid bone uptake accompanied by very rapid blood clearance, which results in a high bone-to-background ratio in a short time. High-quality images of the skeleton can be obtained less than an hour after the intravenous administration of ^{18}F-labeled NaF. ^{18}F-labeled NaF became widely used for skeletal scintigraphy after its introduction by Blau and others in the early 1960s (*2*) and was approved for clinical use by the U.S. Food and Drug Administration in 1972. One limitation of ^{18}F-fluoride scintigraphy was the relatively high energy of the 511-keV annihilation photons produced by decay of ^{18}F. This high energy necessitated imaging with rectilinear scanners equipped with relatively thick NaI(Tl) crystals and precluded the use of Anger-type γ-cameras. This technical limitation, combined with the widespread availability of ^{99}Mo/^{99m}Tc generators, encouraged the development of ^{99m}Tc-labeled bone agents.

In the early 1970s, ^{99m}Tc-labeled polyphosphates and then ^{99m}Tc-labeled pyrophosphate were introduced as bone-imaging agents. With readily available ^{99m}Tc, bone scintigraphy quickly became one of the most commonly performed nuclear medicine imaging procedures (*3*). When it became apparent that pyrophosphate impurities or degradation products were responsible for most of the bone-imaging properties of ^{99m}Tc-labeled polyphosphates, ^{99m}Tc-polyphosphates were abandoned in favor of ^{99m}Tc-pyrophosphate (*4*). However, skeletal imaging with ^{99m}Tc-pyrophosphate was limited by prolonged clearance from the circulation. During this same period, ^{99m}Tc-labeled diphosphonates were introduced for skeletal scintigraphy. These compounds demonstrated higher skeletal uptake, faster blood-pool clearance, and better in vivo stability than did either polyphosphates or pyrophosphate. With the successful development of kit-based ^{99m}Tc-diphosphonate radiopharmaceuticals and the increased availability of Anger-type γ-cameras, ^{99m}Tc-diphosphonates, particularly ^{99m}Tc-methylene diphosphonate (MDP), which demonstrated faster blood-pool clearance than did most other ^{99m}Tc-labeled diphosphonates, became adopted as the standard agent for skeletal scintigraphy (*3,4*). The precipitous decline in the use of ^{18}F-labeled NaF for skeletal scintigraphy did not, therefore, reflect limitations of ^{18}F-labeled NaF as a tracer per se, but instead was the result of, first, the difficulty in imaging 511-keV photons on a system optimized for the 140-keV photons of ^{99m}Tc and, second, the

Received May 4, 2007; revision accepted Sep. 10, 2007.
For correspondence or reprints contact: S. Ted Treves, MD, Children's Hospital Boston, 300 Longwood Ave., PV2C12, Boston, MA 02115.
E-mail: ted.treves@childrens.harvard.edu
*NOTE: FOR CE CREDIT, YOU CAN ACCESS THIS ACTIVITY THROUGH THE SNM WEB SITE (http://www.snm.org/ce_online) THROUGH JANUARY 2009.
No potential conflict of interest relevant to this article was reported.

logistic challenges in the production and efficient delivery of a radioisotope with a physical half-life of 110 min.

In the early 1990s, based on the favorable skeletal kinetics of ^{18}F-fluoride (*5*), Phelps et al. used ^{18}F-fluoride PET as a model for the development of whole-body PET (*6*). Current PET scanners have higher spatial resolution and substantially greater sensitivity than do conventional γ-cameras, resulting in higher image quality for PET (Fig. 1) than for planar scintigraphy or SPECT. Driven by the demand for ^{18}F-FDG, an efficient commercial system now exists for the production and delivery of ^{18}F-labeled NaF. Therefore, because prior technical and logistic limitations to the routine use of ^{18}F-fluoride for bone imaging were no longer present, the increasing availability of PET systems renewed interest in using ^{18}F-labeled NaF as a radiotracer for skeletal imaging.

In the past decade, the clinical utility of ^{18}F-fluoride PET bone scans has been demonstrated by numerous studies, which will be discussed in this review. In these studies, direct comparison with ^{99m}Tc-MDP bone scans has shown ^{18}F-fluoride PET to have a higher diagnostic accuracy in the assessment of malignant and benign skeletal disease. The widespread readoption of ^{18}F-labeled NaF as a bone-imaging agent, however, has been limited by longstanding familiarity with ^{99m}Tc-diphosphonate scintigraphy and, possibly, by concerns about insurance reimbursement for ^{18}F-fluoride PET.

PRODUCTION AND PHARMACOLOGY OF ^{18}F

Historically, one reason for the early interest in ^{18}F-fluoride for bone imaging, other than its high affinity for bone, was that it is relatively easy to produce in high specific activity in a nuclear reactor using a 2-step reaction starting with an Li_2CO_3 target.

$$^{6}\mathrm{Li} + \mathrm{n} \rightarrow {}^{3}\mathrm{H} + {}^{4}\mathrm{He}$$

$$^{3}\mathrm{H} + {}^{16}\mathrm{O} \rightarrow {}^{18}\mathrm{F} + \mathrm{n}$$

The high-energy tritons produced by fission of ^{6}Li react with the ^{16}O from the CO_3^{2-} in the $LiCO_3$ target to produce ^{18}F (*7*). No other fluorine isotopes are produced, so the material is carrier-free. The reaction does, however, produce a significant amount of ^{3}H that must be removed before the tracer can safely be administered to patients. These large amounts of ^{3}H also present a significant radioactive waste disposal problem.

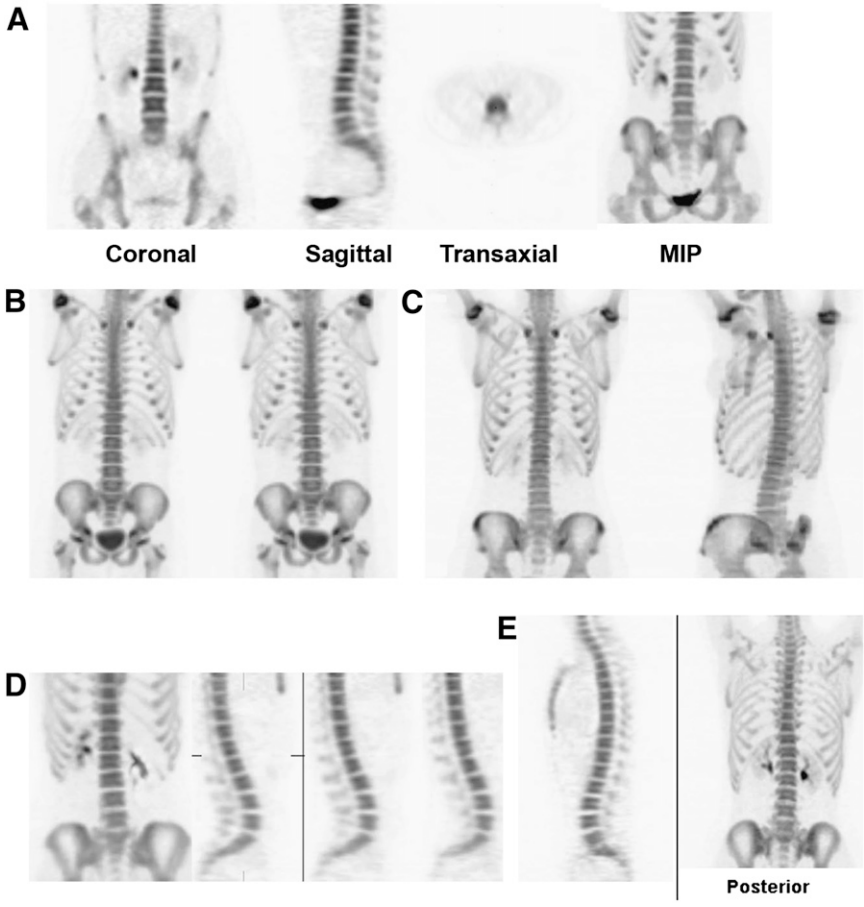

FIGURE 1. Normal ^{18}F-fluoride PET skeletal findings for patients aged 5 y (A), 11 y (B), 15 y (C), 19 y (D), and 30 y (E). Pattern of $^{18}F^-$ uptake in skeleton is similar to pattern seen with more familiar ^{99m}Tc-labeled bisphosphonate bone scans and illustrates changes that occur with maturation of skeleton. Compared with ^{99m}Tc-MDP SPECT, ^{18}F-fluoride bone PET provides higher-quality images, better ratios of bone uptake to soft-tissue uptake, and shorter studies. MIP = maximum-intensity projection.

Currently, nearly all ^{18}F used for clinical applications is produced in a cyclotron using a 1-step reaction with isotopically enriched (≥95%) $^{18}OH_2$ (water) as the target (*8*):

$$^{18}O + p \rightarrow {}^{18}F + n$$

Several curies of ^{18}F can be produced using short irradiation times (2 h) with beam currents that are achievable with clinical cyclotrons. The ^{18}F that is produced in this reaction is collected as $^{18}F^-$ by passage of the irradiated water through an ion-exchange column. If the $^{18}F^-$ is to be used for bone scanning, no further chemical processing is required.

After intravenous administration, ^{18}F-fluoride is rapidly cleared from the plasma in a biexponential manner. The first phase has a half-life of 0.4 h, and the second phase has a half-life of 2.6 h (*9*). Essentially all the ^{18}F-fluoride that is delivered to bone by the blood is retained in the bone (*10*). Tracer retention by the bone is a 2-phase process (*11*). In the first phase, the $^{18}F^-$ ion exchanges for an OH^- ion on the surface of the hydroxyapatite matrix of bone. In the second phase, the $^{18}F^-$ ion migrates into the crystalline matrix of bone, where it is retained until the bone is remodeled. One hour after administration of ^{18}F-labeled NaF, only about 10% of the injected dose remains in the blood (*1*).

Approximately 30% of the injected dose of ^{18}F-fluoride is sequestered within circulating red blood cells. However, ^{18}F-fluoride is freely diffusible from the red cells to the bone surface; moreover, red blood cell uptake does not appear to interfere with uptake of the tracer by bone (*12*). The total uptake of ^{18}F-fluoride by the bone is similar to that of ^{99m}Tc-MDP, at approximately 50% of the injected dose (*13*). There is minimal binding of ^{18}F-fluoride by serum proteins (*12*). This is an important difference between ^{18}F-fluoride and ^{99m}Tc-MDP and other ^{99m}Tc-diphosphonate bone agents, all of which show significant protein binding. Approximately 30% of ^{99m}Tc-MDP is protein-bound immediately after injection; this fraction increases to approximately 70% by 24 h after injection (*14*). The non–protein-bound fraction of ^{99m}Tc-MDP is rapidly cleared from the blood with a half-life similar to that of ^{18}F-fluoride, but the protein-bound fraction is cleared much more slowly (*15*). Hence, it is necessary to wait 3–4 h after injection of ^{99m}Tc-MDP before imaging. By comparison, imaging can be performed less than 1 h after ^{18}F-labeled NaF administration.

CLINICAL USE OF ^{18}F-FLUORIDE: ONCOLOGY

One of the first well-described applications of ^{18}F-fluoride PET was the imaging of primary bone tumors. Using projection and tomographic images, both malignant and benign skeletal lesions were identified by ^{18}F-fluoride PET in 18 subjects (*6,16*). Subsequent clinical use has demonstrated the utility of ^{18}F-fluoride PET in detecting primary bone tumors (Fig. 2).

^{18}F-Fluoride PET also has been used to identify skeletal metastasis in patients with a range of primary tumors. In a study of 5 breast cancer patients with multiple skeletal metastases, increased ^{18}F-fluoride uptake was seen both in lesions with sclerotic characteristics on CT and in lytic lesions, but there was no apparent correlation between the intensity of uptake and the amount of bone matrix seen on CT. Lesions measuring less than 3 mm on CT had limited detectability on ^{18}F-fluoride PET. No formal comparison was made between ^{99m}Tc bone scintigraphy and ^{18}F-fluoride PET (*17*).

FIGURE 2. In 8-y-old patient with Ewing's sarcoma of right distal fibula, ^{18}F-fluoride PET projection image shows extent of primary tumor and absence of skeletal metastases.

In 2 reports, Schirrmeister et al. compared ^{18}F-fluoride PET and planar ^{99m}Tc-MDP scintigraphy in the detection of skeletal metastases in patients with a variety of solid tumors (*18,19*). Lesions were characterized as benign or malignant based on appearance on bone scans; additional imaging, including CT, MRI, and ^{131}I scintigraphy; and clinical follow-up. In 44 patients with prostate, lung, or thyroid cancer, ^{18}F-fluoride PET detected 96 metastatic lesions in 15 patients, whereas ^{99m}Tc-MDP planar scintigraphy detected only 46 metastases (*18*). Although ^{18}F-fluoride PET detected all the lesions identified by ^{99m}Tc-MDP planar scintigraphy, ^{99m}Tc-MDP found only 40% of spine metastases and 82.8% of lesions identified as metastatic in the skull, chest, and extremities. In 34 patients with known or suspected metastatic breast cancer, ^{18}F-fluoride PET detected 64 metastatic lesions in 17 patients, whereas ^{99m}Tc-MDP scintigraphy correctly identified only 29 metastases in 11 patients (*19*). One lesion that was later shown to be metastatic was interpreted as equivocal on ^{18}F-fluoride PET, whereas 14 metastatic lesions were characterized as equivocal or benign by ^{99m}Tc-MDP scintigraphy. Tc-MDP SPECT was performed on a subset of 12 patients but did not identify any additional metastatic lesions. Clinical management was changed in 4 patients in whom previously undetected bone metastases were found by ^{18}F-fluoride PET (*19*). Because ^{18}F-fluoride PET was compared primarily to whole-body ^{99m}Tc-MDP planar imaging, these 2 studies could not establish whether the increased sensitivity of ^{18}F-fluoride PET reflected increased sensitivity of ^{18}F-fluoride as a radiotracer or the improved performance of tomographic imaging.

When ^{18}F-fluoride PET was prospectively compared with ^{99m}Tc-MDP planar scintigraphy and SPECT in a cohort of

53 patients with small cell or non–small cell lung cancer and without previously known metastatic disease, skeletal metastases were identified in only 12 individuals; in the other 41 patients, no skeletal metastases were identified by any of the bone scans or by MRI of the entire spine (*20*). For the 12 patients who did have skeletal metastases, the combination of ^{99m}Tc-MDP planar images and SPECT outperformed ^{99m}Tc-MDP planar imaging alone. ^{99m}Tc-MDP planar scintigraphy identified metastatic disease in only 5 patients, whereas the addition of ^{99m}Tc-MDP SPECT identified vertebral metastases in an additional 5 patients. For 2 patients in whom the combination of ^{99m}Tc-MDP planar scintigraphy and SPECT was equivocal or negative, ^{18}F-fluoride PET correctly identified metastatic disease, and in 1 patient, these findings resulted in a change in clinical management. In no patients did ^{99m}Tc-MDP identify metastases that were not seen on ^{18}F-fluoride PET.

In another prospective study of an additional 103 patients at the same institution with a new diagnosis of either non–small cell (73 patients) or small cell (30 patients) lung cancer, skeletal metastases were found by MRI in 33 patients (*21*). ^{18}F-Fluoride PET identified metastatic disease in 31 of these patients, 2 more patients than were identified by ^{99m}Tc-MDP planar imaging and SPECT. Two patients with negative findings on ^{18}F-fluoride PET were found to have metastatic disease by MRI of the spine, but in another 2 patients with negative findings on ^{18}F-fluoride PET, MRI findings that initially suggested metastatic disease were later determined to be benign—by autopsy in one and by clinical follow-up in the other. Compared with ^{18}F-fluoride PET, ^{99m}Tc-MDP SPECT underestimated the extent of disease in 16 patients, which was nearly half the total number of patients with skeletal metastases. As a result of ^{18}F-fluoride PET findings that were not identified on ^{99m}Tc-MDP SPECT, the clinical management of 2 patients was changed. ^{18}F-Fluoride PET also demonstrated fewer indeterminate lesions than did ^{99m}Tc-MDP SPECT. Only 3 indeterminate lesions, 1 of which represented skeletal metastatic disease, were found on ^{18}F-fluoride PET, compared with 13 indeterminate lesions, 3 of which were subsequently identified as skeletal metastases, on ^{99m}Tc-MDP SPECT. As an additional part of this study, ^{18}F-FDG PET was performed on 41 patients and detected skeletal metastases in 8 of 10 patients in whom skeletal metastases previously had been identified by ^{18}F-fluoride PET. The relative roles of ^{18}F-FDG and ^{18}F-fluoride in imaging skeletal metastases must be better defined, because little has been published comparing ^{18}F-labeled NaF and ^{18}F-FDG or other PET radiopharmaceuticals. Hoegerle has proposed the combined administration of ^{18}F-FDG and ^{18}F-labeled NaF, but this approach has not been widely adopted (*22*). In a report of 20 patients with a wide range of primary tumors, many skeletal metastases were detected by both radiopharmaceuticals (*23*). ^{18}F-FDG was more likely to detect bone marrow metastases or small osteolytic lesions, presumably lesions with little or no increase in cortical bone turnover. ^{18}F-labeled NaF was more likely to detect skeletal metastases of tumors that typically have low FDG avidity, such as thyroid cancer or renal cell cancer (Fig. 3).

The rapid assimilation of PET/CT only a few years after the introduction of ^{18}F-FDG PET into routine clinical practice means that hybrid imaging is now also widely available for ^{18}F-fluoride PET. Two publications from the same institution compared the accuracy of ^{18}F-fluoride PET and ^{18}F-fluoride PET/CT in detecting skeletal metastases (*24,25*). In 44 patients with a variety of primary tumors, ^{18}F-fluoride PET/CT was used to evaluate skeletal pain in the absence of findings on analysis of 198 of the lesions by ^{99m}Tc-MDP scintigraphy. One hundred eleven of 212 skeletal lesions were characterized as metastatic based on analysis of 198 of the lesions by histopathology (9), contemporaneous CT or MRI (64), or imaging and clinical follow-up (125). Nearly all ^{18}F-fluoride–avid lesions (85 of 89) characterized as benign had been identified as benign on the initial CT scan, demonstrating a higher specificity for ^{18}F-fluoride PET/CT than for ^{18}F-fluoride PET. Among the 18 patients not diagnosed with skeletal metastases, 16 had at least 1 focus of ^{18}F-fluoride uptake that corresponded with

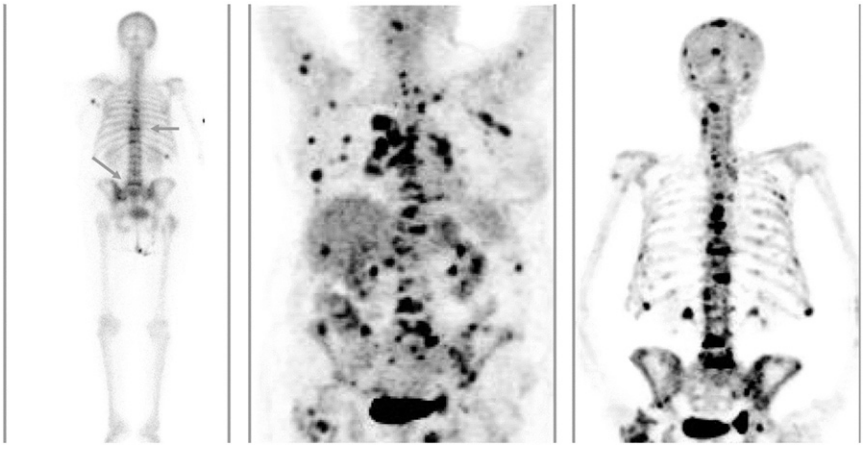

FIGURE 3. Compared with ^{99m}Tc-MDP scintigraphy (left, arrows indicate sites of thoracic and lumbar spine disease), both ^{18}F-FDG PET (middle) and ^{18}F-fluoride PET (right) show higher sensitivity for detecting skeletal lesions. Compared with ^{18}F-FDG PET, ^{18}F-fluoride PET demonstrates minimal soft-tissue uptake, which increases sensitivity for detecting bone lesions that are adjacent to sites of physiologic ^{18}F-FDG uptake or sites of ^{18}F-FDG–avid soft-tissue disease (Reprinted with permission of (*23*).).

a benign finding on CT (*24*). One issue not addressed in this study, however, is the likelihood that patients referred specifically for skeletal symptoms may be more likely to have an increased incidence of benign ^{18}F-fluoride–avid skeletal findings.

In a subsequent prospective study, planar and SPECT ^{99m}Tc-MDP bone scans, ^{18}F-fluoride PET, and ^{18}F-fluoride PET/CT were performed on 44 patients with high-risk prostate cancer, and 23 patients were characterized as having metastatic disease (Fig. 4) (*25*). In 20 patients, ^{18}F-fluoride PET/CT findings were used as the final determinant of whether a lesion was metastatic or benign. In 3 patients with ^{18}F-fluoride–avid lesions, but nondiagnostic CT and MRI findings, bone biopsy (1 patient) or progression of disease on subsequent imaging (2 patients) was used to establish the diagnosis of metastases. The 21 patients in whom metastatic disease was not diagnosed on ^{18}F-fluoride PET/CT had no clinical or imaging evidence of metastases during at least 6 mo of follow-up. As was the case in prior studies, ^{18}F-fluoride PET was more sensitive in detecting skeletal metastases than was planar ^{99m}Tc-MDP scintigraphy either alone or in combination with ^{99m}Tc-MDP SPECT. ^{18}F-Fluoride PET detected skeletal metastases in all 23 patients, whereas ^{99m}Tc-MDP imaging detected lesions in only 18 patients. In a subset of 24 patients (13 with metastases on PET/CT and 11 without metastatic disease), ^{99m}Tc-MDP SPECT was performed of the whole body and not just 1 field of view. Whole-body ^{99m}Tc-MDP SPECT detected metastatic disease in 12 of 13 patients, whereas ^{18}F-fluoride PET identified metastases in all 13 patients. However, in the absence of correlative CT scans, ^{18}F-fluoride PET and combined planar imaging and SPECT with ^{99m}Tc-MDP had similar specificities. No assessment was made as to whether hybrid ^{18}F-fluoride PET/CT was more accurate than a correlation of separately obtained ^{18}F-fluoride PET and CT studies in identifying skeletal metastases. However, as PET/CT scanners replace stand-alone PET systems, this question may become less of an issue.

^{18}F-Fluoride uptake also parallels ^{99m}Tc-MDP uptake in other clinical oncologic disorders. Soft-tissue uptake interpreted as extraosseous ossification has been detected by ^{18}F-fluoride PET, including presumed pulmonary metastases of osteosarcoma and neuroblastoma (Fig. 5) (*6,16*). A recent case report describes a posttreatment flare phenomenon characterized by transient ^{18}F-fluoride uptake at a site of decreased ^{18}F-FDG uptake after a recent change in breast cancer therapy (*26*). As the use of ^{18}F-fluoride PET in oncology patients becomes more common, much of the clinical experience acquired with ^{99m}Tc-MDP scintigraphy should prove applicable to ^{18}F-fluoride PET.

CLINICAL USE OF ^{18}F-FLUORIDE: BENIGN DISEASES OF THE SKELETON

Skeletal scintigraphy has become an important part of evaluating back pain in children and adolescents, particularly in young athletes (*27*). Two recent reports have described the utility of ^{18}F-fluoride PET in the evaluation of these patients (*28,29*). In one report, ^{18}F-fluoride PET/CT was performed on 15 young patients (aged 9–19 y) with back pain (*28*). Nine of the 15 patients had abnormal ^{18}F-fluoride uptake in the spine or pelvis that correlated with abnormal CT findings. Two patients, found on CT to have herniated disks but no osseous abnormalities, did not demonstrate corresponding ^{18}F-fluoride uptake. No sites of abnormal ^{18}F-fluoride uptake without a corresponding CT finding were identified. In another report (Figs. 6–8), 94 patients (aged 4–26 y) with back pain were evaluated with ^{18}F-fluoride PET (*29*). Abnormal focal ^{18}F-fluoride uptake was identified in the spines of 52 of these patients, with 15 patients having more than one site of abnormal uptake. Additional correlative imaging, such as CT, was not performed in the absence of other indications, but the ^{18}F-fluoride PET findings were used by the referring physicians to guide patient treatment. More recently, the use of PET/CT image fusion has improved localization and characterization of lesions identified on bone ^{18}F-fluoride PET (Fig. 8).

As with skeletal SPECT, ^{18}F-fluoride PET is a sensitive method for the detection of focal changes in bones secondary to stress caused by intense sports activity. In our experience,

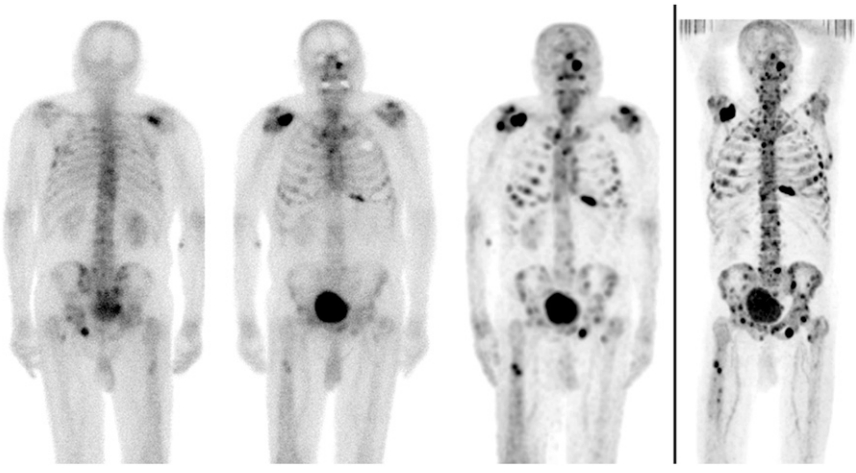

FIGURE 4. From left to right: posterior and anterior ^{99m}Tc-MDP planar scintigraphy, ^{99m}Tc-MDP multiple-field-of-view SPECT, and ^{18}F-fluoride PET of 82-y-old patient with numerous bone metastases. As in this patient, more lesions are typically detected by SPECT than by planar imaging, and ^{18}F-fluoride PET detects more lesions than does SPECT.

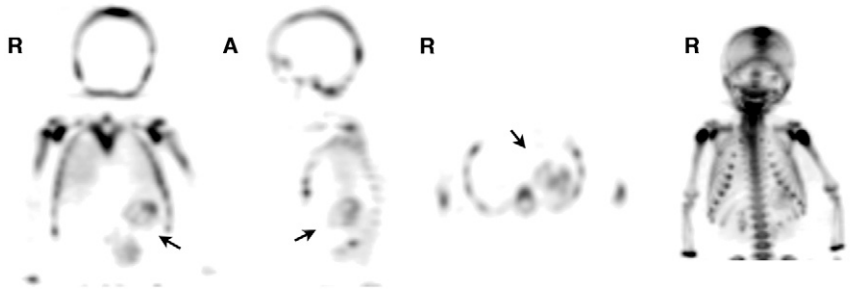

FIGURE 5. In 2-y-old girl with stage IV neuroblastoma, uptake in multiple soft-tissue tumors on ^{18}F-fluoride PET bone scan demonstrates ^{18}F-fluoride avidity for sites of soft-tissue calcification. A = anterior; R = right.

only about half of patients who showed focal ^{18}F-fluoride uptake in a posterior element of the lumbar spine had accompanying CT evidence of spondylolysis. Of cases in which ^{18}F-fluoride PET findings were normal, CT confirmed the absence of abnormality in two thirds and detected pars fracture of indeterminate age in one third. The focal increase of tracer uptake in a pars interarticularis is not necessarily associated with fracture; in some cases, the increase might represent only increased bone turnover due to stress. Depending on the age of the lesion, a pars fracture may or may not show an associated focal increase of ^{18}F-fluoride uptake. Early or active lesions will show increased tracer uptake. However, older, well-established pars fractures, presumably with little active healing or bone remodeling, may not necessarily show increased tracer uptake in the region of interest.

Skeletal ^{18}F-fluoride PET also has been used to predict bone viability after trauma or reconstructive surgery. In 5 patients with hip fracture and clinical concern about osteonecrosis, dynamic ^{18}F-fluoride PET was used to measure bone blood flow and assess the extent of viable bone in the femoral head (*30*). Either impaired blood flow or decreased ^{18}F-fluoride influx predicted an eventual need for joint replacement surgery. In 10 patients who had undergone resurfacing arthroplasty of the hip, ^{18}F-fluoride PET was used to demonstrate normal ^{18}F-fluoride uptake in bone underlying the resurfacing prosthesis (*31*). In patients undergoing hip revision arthroplasty for prosthesis loosening, allogenic bone grafts may be required to stabilize the hip joint. Two reports have described the use of ^{18}F-fluoride PET to assess bone graft viability. In 16 patients, dynamic ^{18}F-fluoride PET was performed either early (3–6 wk) or late (9 mo–5 y) after surgery (*32*). Early studies demonstrated similar uptake in both allograft bone and adjacent cortical bone, whereas later studies showed less activity in allograft bone than in cortical bone. Another report describes 5 patients on whom dynamic ^{18}F-fluoride PET was performed both early (1–8 d) and late (1 y) after surgery (*33*). Three of the 5 patients also were studied 4 mo after surgery.

In certain clinical settings, one potential limitation of ^{18}F-fluoride PET is the inability to yield an equivalent to a 3-phase bone scan. ^{18}F-Fluoride would not be expected to accumulate in acute inflammatory processes in soft tissue and so will not be useful to image processes that can be identified on tissue-phase images of ^{99m}Tc-MDP scintigraphy. Concurrent or sequential use of ^{18}F-labeled NaF and ^{18}F-FDG may be an approach to assessing soft tissue adjacent to a skeletal lesion. It is possible that ^{99m}Tc-diphosphonates will continue to have a role in clinical situations requiring a 3-phase bone scan.

Several investigators have used ^{18}F-fluoride skeletal PET to quantitatively assess bone turnover. Quantitative ^{18}F-fluoride PET provides a noninvasive measure of bone turnover that correlates with bone histomorphometry (*34,35*). The use of quantitative ^{18}F-fluoride PET has been demonstrated in patients with renal osteodystrophy (*34*), postmenopausal osteoporosis (*36*), and Paget's disease (*37*). For example, in a study of 11 patients with renal osteodystrophy, the calculated rate constant of net incorporation of ^{18}F-fluoride into bone was similar when calculated by either a 3-compartment model or Patlak analysis and correlated with serum markers of bone turnover (e.g., alkaline phosphatase) and PTH level (*34*). The rate of fluoride incorporation into bone also correlated with histomorphometric indices of bone turnover in iliac crest biopsies and was higher in patients with high-turnover osteodystrophy than in patients with low-turnover bone disease or in healthy subjects. Although useful as a research tool to help improve the understanding of bone metabolism, ^{18}F-fluoride PET has not entered routine clinical practice for the diagnosis and assessment of metabolic bone disease or osteoporosis.

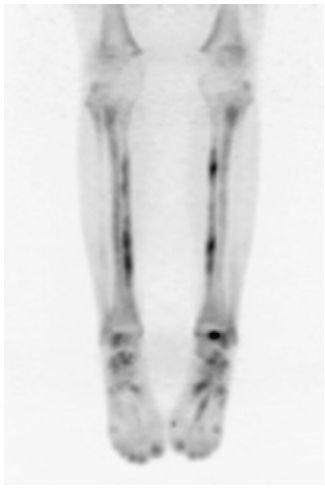

FIGURE 6. In 18-y-old female marathon runner with severe lower leg and foot pain, projection PET image shows increased ^{18}F-fluoride uptake in tibiae and both feet, indicating multiple sites of stress injury.

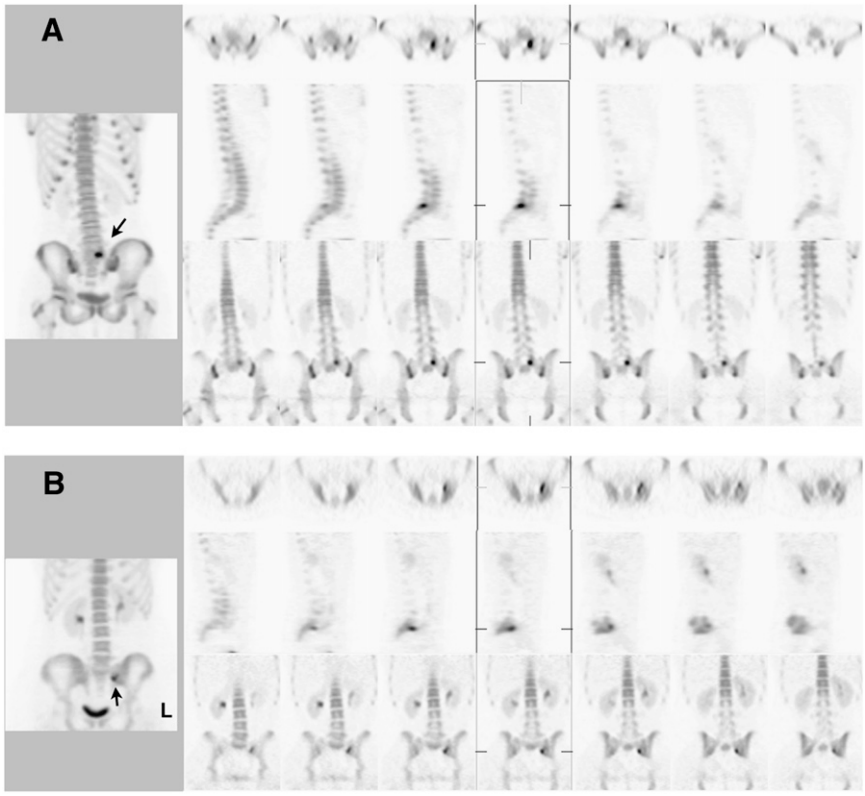

FIGURE 7. (A) In 12-y-old female gymnast with lower back pain, ^{18}F-fluoride PET image shows increased focal uptake indicating stress changes in posterior elements of L5 vertebra (arrow). (B) In 21-y-old runner, ^{18}F-fluoride PET image shows stress changes in left sacroiliac region (arrow).

DOSIMETRY

Several factors affect the radiation dose of ^{18}F relative to that of single-photon emitters (such as ^{99m}Tc). With a positron emitter such as ^{18}F, energy is delivered by the positron itself (mean energy, 250 keV) and by the two 511-keV annihilation photons, whereas ^{99m}Tc emits a single 140-keV γ-ray, as well as conversion electrons in low abundance. These differences affect the relative internal dosimetry of ^{18}F and ^{99m}Tc. The ^{18}F positron will deposit essentially all its kinetic energy in the source organ, whereas the different energies of 511-keV and 140-keV photons result in different patterns of internal radiation dose. The soft-tissue half-value layers for the 511- and 140-keV photons are 7.3 and 4.6 cm, respectively, so that 511-keV photons can deliver their energy to organs distant from the source organ, whereas the 140-keV photons will deliver more of their energy to organs near the source organ. On the other hand, the half-life for ^{18}F is 110 min, compared with 6 h for ^{99m}Tc, leading to a shorter exposure period and, in turn, to a reduced radiation dose for ^{18}F.

With consideration of all these factors, the radiation dosimetry for both ^{18}F-labeled NaF and ^{99m}Tc-MDP was calculated using the data provided by reports 53 and 80, respectively, of the International Commission on Radiological Protection (ICRP) (*38,39*). The effective doses per unit of administered activity for ^{18}F-labeled NaF and ^{99m}Tc-MDP were calculated, as was the radiation dose to several individual organs (Table 1). Also listed in this table are the absolute doses for patients of different sizes for injected activities of 2.11 and 7.40 MBq/kg for ^{18}F-labeled NaF and ^{99m}Tc-MDP, respectively. At the prescribed administered activities, the effective dose for ^{18}F-labeled NaF and ^{99m}Tc-MDP are similar for most patients (4.0 and 3.0 mSv, respectively, for a 70-kg patient). For patients weighing less than 20 kg, the effective dose is relatively less with ^{99m}Tc-MDP (2.0 mSv) than with ^{18}F-labeled NaF (approximately 3.5 mSv). The bone surface dose is higher for ^{99m}Tc-MDP relative to that for ^{18}F-labeled NaF (32.6 and 5.9 mGy, respectively, for a 70-kg patient), whereas the dose to the bladder wall is slightly higher for ^{18}F-labeled NaF than for ^{99m}Tc-MDP (32.6 and 24.9 mGy, respectively, for a 70-kg patient). Therefore, there is little overall difference in the estimated radiation dose for ^{18}F-labeled NaF PET and ^{99m}Tc-MDP scintigraphy.

TECHNICAL ASPECTS

Some commercial PET scanners allow data to be acquired in either 2-dimensional mode (interplane septa in place) or 3-dimensional mode (interplane septa removed). Because ^{18}F-fluoride is well localized within the skeleton, excellent image quality can be obtained with either mode. The higher sensitivity of 3-dimensional PET allows the injected activity to be kept at a level (e.g., 2.1 MBq/kg) that yields a radiation dose to the patient similar to that received from ^{99m}Tc-MDP (Table 1). Moreover, the rapid uptake in bone and fast clearance from soft tissue of ^{18}F-fluoride allows data recording to commence 15–30 min after intravenous

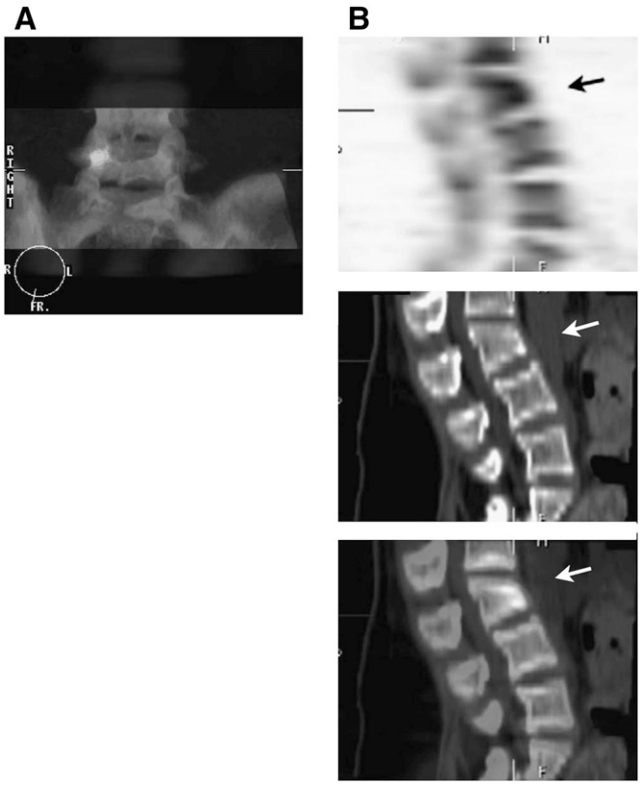

FIGURE 8. (A) Fusion of ^{18}F-fluoride PET and CT images of 17-y-old male athlete with back pain that worsened on hyperextension. ^{18}F-Fluoride PET had identified focally increased tracer uptake in region of right pars interarticularis of L5 vertebra. Fusion image demonstrates correlation of site of $^{18}F^-$ uptake with nondisplaced fracture of pars that was identified by CT. (B) From top to bottom, sagittal ^{18}F-fluoride PET, CT, and fusion images of 15-y-old female athlete with back pain after landing from high jump. Increased ^{18}F-fluoride uptake and deformity on PET correlates to wedge compression fracture of L3 vertebra (arrows) identified on CT.

administration of the radiopharmaceutical. Because modern PET scanners have axial fields of view of 15–20 cm, multiple bed positions will likely be required to adequately image the area of interest. If the area of concern is localized (e.g., an area of a suspected spinal injury), then 1 or 2 bed positions may be all that is required. In other cases (e.g., an oncologic survey scan), an extended study covering most or all of the skeleton may be required. Acquisition times of 3–5 min per bed position may be applied, depending on the sensitivity of the specific PET scanner being used, the administered activity, and whether the data are being acquired in 2-dimensional or 3-dimensional mode. Routine approaches to PET reconstruction such as filtered backprojection, or iterative approaches such as ordered-subset expectation maximization, can be effectively used with these data. In general, the same reconstruction parameters used for ^{18}F-FDG studies also can be used for ^{18}F-labeled NaF studies, although higher-frequency filtration also may be considered because of the high uptake of radioactivity and the fine spatial detail being imaged.

Because ^{18}F-fluoride is well localized within the skeleton, excellent images can be reconstructed without the use of attenuation correction. The extent of the radioactivity in the transverse plane, whether in the spine or in long bones, is typically small, creating little variation in the intensity of the signal because of photon attenuation. However, failure to use attenuation correction sometimes may lead to artifacts in the reconstructed data (Fig. 9). Although the extent of the activity may be small in the transverse plane, the extent may be quite large in the axial direction. Thus, attenuation can vary significantly when either sagittal or coronal slices are being viewed. Further, without attenuation correction, the thoracic spine will appear to have substantially more uptake than the lumbar spine because the lungs produce less photon attenuation than does soft tissue. Urinary accumulation and excretion of ^{18}F-fluoride can result in image artifacts. Tracer accumulation in the bladder could obscure lesions in the sacrum or pelvis. Thus, as with ^{99m}Tc-MDP bone scans, it is helpful to have the patient void just before imaging. Accumulation of ^{18}F-fluoride in the renal pelvis can produce a signal that is more intense than the signal in adjacent spine. Without attenuation correction, this tracer accumulation may produce streak artifacts. These artifacts result when the signal is attenuated in the right–left direction substantially more than in the anterior–posterior direction, limiting the ability of the reconstruction algorithm to adequately compensate for these streak artifacts. This effect can cause a substantial reduction in the PET signal in the adjacent spine, even when an iterative reconstruction algorithm such as ordered-subset expectation maximization is used (*29*). The application of attenuation correction yields projection data that have more angular uniformity. Calculated or measured attenuation correction using either rotating rods or CT-based attenuation correction will alleviate these artifacts. Thus, the decision to use attenuation correction may depend on which regions of the body are being imaged.

In some applications, the quantitative capability of PET may add value to an image. The capability to report the absolute uptake of ^{18}F-fluoride is the result of the more straightforward attenuation correction for PET and the ability to calibrate the PET scanner to measure absolute activity concentration (in Bq/cm^3). By comparison, SPECT typically provides only relative quantitation of radiopharmaceutical uptake. The quantitative capability of ^{18}F-fluoride PET may prove particularly useful if the clinical interpretation depends on comparison to known standard levels of metabolic activity or on quantitative comparison to a prior study.

PRACTICAL ISSUES

The imaging time required for ^{18}F-fluoride PET is significantly shorter than that required for ^{99m}Tc-diphosphonate scintigraphy. The average time from injection to imaging with ^{18}F-labeled NaF is 15–30 min, compared with 3–4 h for ^{99m}Tc-MDP. Additionally, the total imaging time for ^{18}F-fluoride PET is 15–30 min, whereas a ^{99m}Tc-MDP

TABLE 1
Radiation Dosimetry of ^{99m}Tc-MDP Scintigraphy vs. ^{18}F-Labeled NaF PET

Type of imaging	Adult (70 kg)	15-y-old child (55 kg)	10-y-old child (32 kg)	5-y-old child (19 kg)	1-y-old child (9.8 kg)
^{99m}Tc-MDP*					
Administered activity (MBq)	518	407	237	141	73
Effective dose in mSv/MBq (mSv)	0.0057 (3.0)	0.0070 (2.8)	0.0110 (2.6)	0.0140 (2.0)	0.0270 (2.0)
Bladder wall in mGy/MBq (mGy)	0.048 (24.9)	0.060 (24.4)	0.088 (20.9)	0.073 (10.3)	0.130 (9.5)
Bone surfaces (mGy)	0.063 (32.6)	0.082 (33.4)	0.130 (30.8)	0.220 (31.0)	0.53 (38.7)
Red marrow (mGy)	0.0092 (4.8)	0.010 (4.1)	0.017 (4.0)	0.033 (4.7)	0.067 (4.9)
^{18}F-labeled NaF†					
Administered activity (MBq)	148	116	68	40	21
Effective dose in mSv/MBq (mSv)	0.027 (4.0)	0.034 (3.9)	0.052 (3.5)	0.086 (3.4)	0.170 (3.6)
Bladder wall in mGy/MBq (mGy)	0.22 (32.6)	0.27 (31.3)	0.40 (27.2)	0.61 (24.4)	1.10 (23.1)
Bone surfaces in mGy/MBq (mGy)	0.040 (5.9)	0.050 (5.8)	0.079 (5.4)	0.130 (5.2)	0.300 (6.3)
Red marrow in mGy/MBq (mGy)	0.040 (5.9)	0.053 (6.1)	0.088 (6.0)	0.180 (7.2)	0.380 (8.0)

*Derived from ICRP Report 80. *Ann ICRP.* 1999;28:75.
†Derived from ICRP Report 53. *Ann ICRP.* 1987;17:74.
Values in parentheses are doses in mGy (mSv for effective dose) for administered activity listed in table for that patient size.

SPECT scan takes an average of 60 min. In general, the total examination time is approximately 1 h for ^{18}F-fluoride PET, compared with approximately 4 h for ^{99m}Tc-MDP bone scintigraphy. Moreover, the reduced imaging time associated with ^{18}F-fluoride PET minimizes the opportunity for patient motion and resulting imaging artifacts. However, if motion artifacts do occur, software correction cannot be performed with PET images, as sometimes is possible with SPECT. The use of PET may raise the question of sedation in young children to reduce patient motion. In our department, with skilled nuclear medicine technologists and the assistance of a trained child life specialist, sedation is rarely necessary for ^{99m}Tc-MDP SPECT bone scans. With shorter scan times, sedation is even less likely to be needed with ^{18}F-fluoride PET.

Both the patient and the referring physician benefit from shorter examination times, which are more convenient, pose less physical and emotional stress, and accelerate diagnosis and treatment. With the more rapid turnaround of ^{18}F-fluoride PET results, the patient can easily return the same day to discuss results with the referring physician. The shorter imaging time for ^{18}F-fluoride PET also improves workflow efficiency and resource use. For example, ^{18}F-fluoride PET can be scheduled in any available 1-h opening in the PET schedule, freeing an additional hour of γ-camera imaging time for other scintigraphic studies. At present, the cost per dose of ^{18}F-labeled NaF is higher than that of ^{99m}Tc-MDP, but this difference is at least partially offset by the fewer resources needed for shorter imaging times. In addition, as with ^{18}F-FDG, the unit dose cost of ^{18}F-labeled NaF is likely to decrease as demand increases and the overall market for ^{18}F-labeled NaF grows.

At present, ^{18}F-fluoride PET typically is not performed outside large medical centers because of widespread uncertainty about insurance reimbursement. Although U.S. Food and Drug Administration approval and accepted clinical use of ^{18}F-labeled NaF for skeletal imaging predates those of ^{99m}Tc diphosphonates, many insurance guidelines lack a description of ^{18}F-fluoride bone imaging with any camera type, and most insurance coverage for tomographic imaging is limited to ^{99m}Tc-diphosphonate SPECT. Further contributing to these obstacles is the lack of a Current Procedural Terminology code for ^{18}F-fluoride PET for bone imaging. Assignment of such a Current Procedural Terminology code should facilitate efforts to encourage individual insurance companies to develop specific guidelines for reimbursement.

CONCLUSION

^{18}F-labeled NaF, although one of the early bone-scanning agents, was displaced by the arrival of ^{99m}Tc-labeled bone-imaging agents, which were available in convenient kit form for labeling with generator-produced ^{99m}Tc and produced better images on the commonly used, Anger-style, γ-cameras. The widespread availability of modern PET scanners permits high-quality skeletal imaging with ^{18}F-fluoride, which has the favorable characteristics of highly specific bone uptake, rapid clearance from the blood pool because of minimal protein binding, and dosimetry similar to that of ^{99m}Tc-MDP. The commercial delivery system used for ^{18}F-FDG also can be used for the efficient delivery of other ^{18}F-labeled radiopharmaceuticals, such as ^{18}F-labeled NaF. It is now feasible to perform high-quality ^{18}F-labeled NaF bone scans in most nuclear medicine departments. Numerous recent studies have compared ^{18}F-fluoride PET to ^{99m}Tc-MDP scintigraphy. These studies have demonstrated that ^{18}F-fluoride PET is more accurate than planar imaging or SPECT with ^{99m}Tc-MDP for localizing and characterizing both malignant and benign bone lesions. The addition of

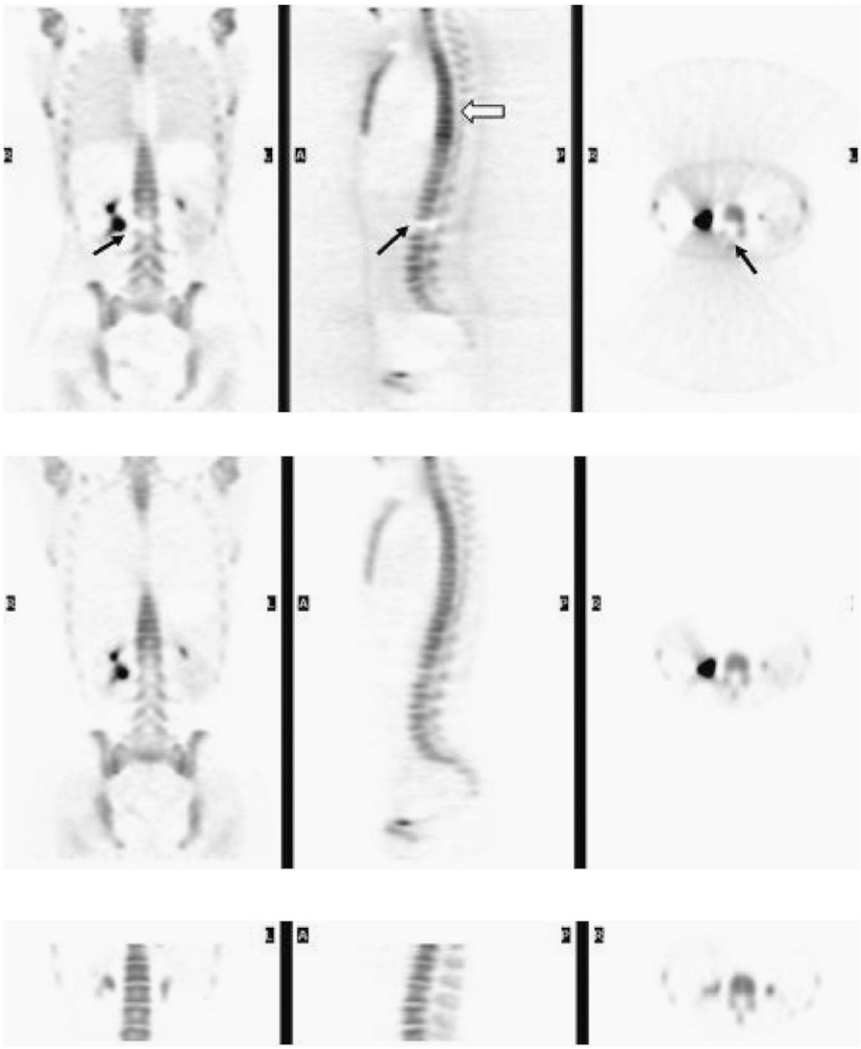

FIGURE 9. In ^{18}F-fluoride PET bone scan without attenuation correction (top row, with coronal, sagittal, and transverse slices appearing from left to right), streak artifact caused by activity in renal collecting system leads to apparent loss of signal in right lumbar spine (solid arrows). Apparent increased signal in thoracic spine results from reduction of attenuation in lung region (open arrow). Both artifacts are greatly reduced when attenuation correction is applied using rotating rod sources of ^{68}Ge/^{68}Ga (middle row). After patient voided, repeated image (bottom row) acquired in single bed position shows resolution of artifact caused by activity in renal collecting system.

correlative imaging, such as CT, MRI, or hybrid imaging with PET/CT, further improves the specificity and accuracy of ^{18}F-fluoride skeletal PET. Direct correlation of ^{18}F-fluoride PET and anatomic imaging using either fusion software or hybrid imaging probably will become the routine clinical practice in nearly all cases. The clinical usefulness of ^{18}F-fluoride PET has been demonstrated for a wide range of clinical indications for oncology and for benign diseases of bone (Table 2).

TABLE 2
Indications for ^{18}F-Fluoride Skeletal PET

Type of disease	Type of assessment	Specific goal
Oncologic	Metastatic disease in skeleton (e.g. prostate, lung, breast, neuroblastoma)	Perform initial evaluation (staging) Assess response of skeletal metastases to therapy Detect skeletal metastases during follow-up
	Bone pain in patients with known cancer	
	Primary bone tumors	Identify sites of disease (initial staging) Assess response to therapy Differentiate postoperative changes from residual/recurrent disease Detect recurrent/metastatic disease during follow-up
Benign bone	Pediatric/young adult back pain	Assess vertebral spondylolysis Assess other stress injuries
	Bone viability	Assess femoral head avascular necrosis Assess bone graft viability (long bones, mandible)
	Paget's disease	Assess extent of disease Monitor response to therapy

Although not yet in routine clinical use, quantitative ^{18}F-fluoride PET may prove useful for the assessment of metabolic bone disorders such as renal osteodystrophy, osteoporosis, or Paget's disease. For many clinical indications, ^{18}F-fluoride PET images can be obtained without attenuation correction, although some well-defined artifacts may be avoided by applying attenuation correction.

^{18}F-Fluoride PET offers the additional advantages of faster study times, improved workflow in the nuclear medicine clinic, increased convenience to the patient, and rapid turnaround of results to the referring physician. The widespread readoption of ^{18}F-labeled NaF as a bone-imaging agent, however, has been limited by longstanding familiarity with ^{99m}Tc-diphosphonate scintigraphy and by issues related to insurance reimbursement for ^{18}F-fluoride PET. The higher-quality imaging, increased clinical accuracy, greater convenience to the patient and referring physician, and more efficient use of nuclear medicine resources all indicate the need to reconsider the use of ^{18}F-fluoride PET for imaging benign and malignant diseases of the skeleton.

ACKNOWLEDGMENTS

We acknowledge the technical support of Stephen Laffin and of the rest of the technical team in the Division of Nuclear Medicine at Children's Hospital Boston. We thank Nancy Drinan and Christopher Durall for editorial assistance in the preparation of the manuscript. Edmond Reidy, Radiology Administrator, helped with the economic assessment.

REFERENCES

1. Blau M, Ganatra R, Bender MA. 18 F-Fluoride for bone imaging. *Semin Nucl Med.* 1972;2:31–37.
2. Blau M, Nagler W, Bender MA. Fluorine-18: a new isotope for bone scanning. *J Nucl Med.* 1962;3:332–334.
3. Thrall JH. Technetium-99m labeled agents for skeletal imaging. *CRC Crit Rev Clin Radiol Nucl Med.* 1976;8:1–31.
4. Davis MA, Jones AG. Comparison of ^{99m}Tc-labeled phosphate and phosphonate agents for skeletal imaging. *Semin Nucl Med.* 1976;6:19–31.
5. Hawkins RA, Choi Y, Huang SC, et al. Evaluation of the skeletal kinetics of fluorine-18-fluoride ion with PET. *J Nucl Med.* 1992;33:633–642.
6. Hoh CK, Hawkins RA, Dahlbom M, et al. Whole body skeletal imaging with [^{18}F]fluoride ion and PET. *J Comput Assist Tomogr.* 1993;17:34–41.
7. Anbar M, Ernst N. A distribution study of F18-labelled cationic fluorocomplexes in rats. *Int J Appl Radiat Isot.* 1962;13:47–51.
8. Ruth TJ, Wolf AP. Absolute cross sections for the production of fluorine-18 via the ^{18}O(p,n)^{18}F reaction. *Radiochimica Acta.* 1979;26:21–24.
9. Weber DA, Greenberg EJ, Dimich A, et al. Kinetics of radionuclides used for bone studies. *J Nucl Med.* 1969;10:8–17.
10. Wootton R, Dore C. The single-passage extraction of ^{18}F in rabbit bone. *Clin Phys Physiol Meas.* 1986;7:333–343.
11. Costeas A, Woodard HQ, Laughlin JS. Depletion of ^{18}F from blood flowing through bone. *J Nucl Med.* 1970;11:43–45.
12. Blake GM, Park-Holohan SJ, Cook GJ, Fogelman I. Quantitative studies of bone with the use of ^{18}F-fluoride and ^{99m}Tc-methylene diphosphonate. *Semin Nucl Med.* 2001;31:28–49.
13. Chilton HM, Francis MD, Thrall JH. Radiopharmaceuticals for bone and bone marrow imaging. In: Swanson DP, Chilton HM, Thrall JH, eds. *Pharmaceuticals in Medical Imaging: Radiopaque Contrast Media, Radiopharmaceuticals, Enhancement Agents for Magnetic Resonance Imaging and Ultrasound.* New York, NY: Macmillan Pub. Co.; 1990:537–563.
14. Hyldstrup L, McNair P, Ring P, Henriksen O. Studies on diphosphonate kinetics. Part I: evaluation of plasma elimination curves during 24 h. *Eur J Nucl Med.* 1987;12:581–584.
15. Park-Holohan SJ, Blake GM, Fogelman I. Quantitative studies of bone using ^{18}F-fluoride and ^{99m}Tc-methylene diphosphonate: evaluation of renal and whole-blood kinetics. *Nucl Med Commun.* 2001;22:1037–1044.
16. Tse N, Hoh C, Hawkins R, Phelps M, Glaspy J. Positron emission tomography diagnosis of pulmonary metastases in osteogenic sarcoma. *Am J Clin Oncol.* 1994;17:22–25.
17. Petren-Mallmin M, Andreasson I, Ljunggren O, et al. Skeletal metastases from breast cancer: uptake of ^{18}F-fluoride measured with positron emission tomography in correlation with CT. *Skeletal Radiol.* 1998;27:72–76.
18. Schirrmeister H, Guhlmann A, Elsner K, et al. Sensitivity in detecting osseous lesions depends on anatomic localization: planar bone scintigraphy versus ^{18}F PET. *J Nucl Med.* 1999;40:1623–1629.
19. Schirrmeister H, Guhlmann A, Kotzerke J, et al. Early detection and accurate description of extent of metastatic bone disease in breast cancer with fluoride ion and positron emission tomography. *J Clin Oncol.* 1999;17:2381–2389.
20. Schirrmeister H, Glatting G, Hetzel J, et al. Prospective evaluation of the clinical value of planar bone scans, SPECT, and ^{18}F-labeled NaF PET in newly diagnosed lung cancer. *J Nucl Med.* 2001;42:1800–1804.
21. Hetzel M, Arslandemir C, Konig HH, et al. F-18 NaF PET for detection of bone metastases in lung cancer: accuracy, cost-effectiveness, and impact on patient management. *J Bone Miner Res.* 2003;18:2206–2214.
22. Hoegerle S, Juengling F, Otte A, Altehoefer C, Moser EA, Nitzsche EU. Combined FDG and [F-18]fluoride whole-body PET: a feasible two-in-one approach to cancer imaging? *Radiology.* 1998;209:253–258.
23. Langsteger W, Heinisch M, Fogelman I. The role of fluorodeoxyglucose, ^{18}F-dihydroxyphenylalanine, ^{18}F-choline, and ^{18}F-fluoride in bone imaging with emphasis on prostate and breast. *Semin Nucl Med.* 2006;36:73–92.
24. Even-Sapir E, Metser U, Flusser G, et al. Assessment of malignant skeletal disease: initial experience with ^{18}F-fluoride PET/CT and comparison between ^{18}F-fluoride PET and ^{18}F-fluoride PET/CT. *J Nucl Med.* 2004;45:272–278.
25. Even-Sapir E, Metser U, Mishani E, Lievshitz G, Lerman H, Leibovitch I. The detection of bone metastases in patients with high-risk prostate cancer: ^{99m}Tc-MDP planar bone scintigraphy, single- and multi-field-of-view SPECT, ^{18}F-fluoride PET, and ^{18}F-fluoride PET/CT. *J Nucl Med.* 2006;47:287–297.
26. Wade AA, Scott JA, Kuter I, Fischman AJ. Flare response in ^{18}F-fluoride ion PET bone scanning. *AJR.* 2006;186:1783–1786.
27. Coady CM, Micheli LJ. Stress fractures in the pediatric athlete. *Clin Sports Med.* 1997;16:225–238.
28. Ovadia D, Metser U, Lievshitz G, Yaniv M, Wientroub S, Even-Sapir E. Back pain in adolescents: assessment with integrated ^{18}F-fluoride positron-emission tomography-computed tomography. *J Pediatr Orthop.* 2007;27:90–93.
29. Lim R, Fahey FH, Drubach LA, Connolly LP, Treves ST. Early experience with ^{18}F sodium fluoride bone PET in young patients with back pain. *J Pediatr Orthop.* 2007;27:277–282.
30. Schiepers C, Broos P, Miserez M, Bormans G, De Roo M. Measurement of skeletal flow with positron emission tomography and ^{18}F-fluoride in femoral head osteonecrosis. *Arch Orthop Trauma Surg.* 1998;118:131–135.
31. Forrest N, Welch A, Murray AD, Schweiger L, Hutchison J, Ashcroft GP. Femoral head viability after Birmingham resurfacing hip arthroplasty: assessment with use of [^{18}F] fluoride positron emission tomography. *J Bone Joint Surg Am.* 2006;88(suppl 3):84–89.
32. Piert M, Winter E, Becker GA, et al. Allogenic bone graft viability after hip revision arthroplasty assessed by dynamic [^{18}F]fluoride ion positron emission tomography. *Eur J Nucl Med.* 1999;26:615–624.
33. Sorensen J, Ullmark G, Langstrom B, Nilsson O. Rapid bone and blood flow formation in impacted morselized allografts: positron emission tomography (PET) studies on allografts in 5 femoral component revisions of total hip arthroplasty. *Acta Orthop Scand.* 2003;74:633–643.
34. Messa C, Goodman WG, Hoh CK, et al. Bone metabolic activity measured with positron emission tomography and [^{18}F]fluoride ion in renal osteodystrophy: correlation with bone histomorphometry. *J Clin Endocrinol Metab.* 1993;77:949–955.
35. Piert M, Zittel TT, Becker GA, et al. Assessment of porcine bone metabolism by dynamic ^{18}F-fluoride ion PET: correlation with bone histomorphometry. *J Nucl Med.* 2001;42:1091–1100.
36. Blake GM, Park-Holohan SJ, Fogelman I. Quantitative studies of bone in postmenopausal women using ^{18}F-fluoride and ^{99m}Tc-methylene diphosphonate. *J Nucl Med.* 2002;43:338–345.
37. Installe J, Nzeusseu A, Bol A, Depresseux G, Devogelaer JP, Lonneux M. ^{18}F-Fluoride PET for monitoring therapeutic response in Paget's disease of bone. *J Nucl Med.* 2005;46:1650–1658.
38. *ICRP Publication 53: Radiation Dose to Patients from Radiopharmaceuticals.* Stockholm, Sweden: International Commission on Radiological Protection; 1987.
39. *ICRP Publication 80: Radiation Dose to Patients from Radiopharmaceuticals.* Stockholm, Sweden: International Commission on Radiological Protection; 1999.